Video Article

# Quantification of Atherosclerotic Plaque Activity and Vascular Inflammation using [18-F] Fluorodeoxyglucose Positron Emission Tomography/Computed Tomography (FDG-PET/CT)

Nehal N. Mehta[1], Drew A. Torigian[2], Joel M. Gelfand[3], Babak Saboury[2], Abass Alavi[2]

[1]Division of Cardiovascular Medicine, University of Pennsylvania, Perelman School of Medicine

[2]Department of Radiology, University of Pennsylvania, Perelman School of Medicine

[3]Department of Dermatology, University of Pennsylvania, Perelman School of Medicine

Correspondence to: Nehal N. Mehta at Nehal.Mehta@uphs.upenn.edu

## Abstract

Conventional non-invasive imaging modalities of atherosclerosis such as coronary artery calcium (CAC)[1] and carotid intimal medial thickness (C-IMT)[2] provide information about the burden of disease. However, despite multiple validation studies of CAC[3-5], and C-IMT[2,6], these modalities do not accurately assess plaque characteristics[7,8], and the composition and inflammatory state of the plaque determine its stability and, therefore, the risk of clinical events[9-13].

[18F]-2-fluoro-2-deoxy-D-glucose (FDG) imaging using positron-emission tomography (PET)/computed tomography (CT) has been extensively studied in oncologic metabolism[14,15]. Studies using animal models and immunohistochemistry in humans show that FDG-PET/CT is exquisitely sensitive for detecting macrophage activity[16], an important source of cellular inflammation in vessel walls. More recently, we[17,18] and others have shown that FDG-PET/CT enables highly precise, novel measurements of inflammatory activity of activity of atherosclerotic plaques in large and medium-sized arteries[9,16,19,20]. FDG-PET/CT studies have many advantages over other imaging modalities: 1) high contrast resolution; 2) quantification of plaque volume and metabolic activity allowing for multi-modal atherosclerotic plaque quantification; 3) dynamic, real-time, *in vivo* imaging; 4) minimal operator dependence. Finally, vascular inflammation detected by FDG-PET/CT has been shown to predict cardiovascular (CV) events independent of traditional risk factors[21,22] and is also highly associated with overall burden of atherosclerosis[23]. Plaque activity by FDG-PET/CT is modulated by known beneficial CV interventions such as short term (12 week) statin therapy[24] as well as longer term therapeutic lifestyle changes (16 months)[25].

The current methodology for quantification of FDG uptake in atherosclerotic plaque involves measurement of the standardized uptake value (SUV) of an artery of interest and of the venous blood pool in order to calculate a target to background ratio (TBR), which is calculated by dividing the arterial SUV by the venous blood pool SUV. This method has shown to represent a stable, reproducible phenotype over time, has a high sensitivity for detection of vascular inflammation, and also has high inter-and intra-reader reliability[26]. Here we present our methodology for patient preparation, image acquisition, and quantification of atherosclerotic plaque activity and vascular inflammation using SUV, TBR, and a global parameter called the metabolic volumetric product (MVP). These approaches may be applied to assess vascular inflammation in various study samples of interest in a consistent fashion as we have shown in several prior publications.[9,20,27,28]

## Video Link

The video component of this article can be found at https://www.jove.com/video/3777/

## Protocol

## 1. Patient Preparation and Obtaining Images

1. Secure at least a one hour imaging time slot on a PET/CT scanner, preferably one with time-of-flight capabilities for improved image quality. At our institution, we use a Gemini TF scanner, which is the newest PET/CT system from Philips Medical Systems and combines a PET scanner based on LYSO detectors with a 16-slice Brilliance CT system.
2. Have subjects fast for 8 hours prior to the FDG-PET/CT scan. Check fasting serum glucose (FSG) levels using a fingerstick to assure serum glucose < 200 mg/dL prior to FDG administration. This ensures that glucose within the body does not compete with FDG.
3. If FSG < 200 mg/dL, insert no smaller than a 20-gauge intravenous (IV) line to administer the radiotracer (FDG) IV. Administer approximately 5.2 MBq/kg of FDG.

4. ~60 minutes after intravenous administration of FDG, perform low dose CT imaging of the whole body. Then acquire PET emission images from the skull vertex to the toes. On the particular PET/CT listed in 1.1), image reconstruction is typically performed using a list-mode maximum-likelihood expectation-maximization (ML-EM) algorithm with 33 ordered subsets and 3 iterations, where the system model includes time-of-flight as well as normalization, attenuation, randoms, and scatter corrections. Rescaled low-dose CT images are utilized for attenuation correction of PET images in an automated fashion, leading to decreased examination time and improved image quality relative to external radioactive source attenuation correction used on PET only machines.

## 2. PET Image Qualitative Evaluation

1. Interpret axial, sagittal, and coronal PET reconstructions with and without attenuation correction using low dose non-contrast CT images for spatial delineation of vascular structures of interest as well as for precise anatomical localization of areas of increased radiotracer uptake seen on PET images.

## 3. PET Image Quantitative Evaluation

1. After qualitative review of the images, identify boundaries to divide the aorta into the following sections: ascending aorta, aortic arch, descending thoracic aorta, suprarenal abdominal aorta, and infrarenal abdominal aorta. For simplicity, the aortic arch can be defined by those portions of the thoracic aorta that appear as a contiguous segment on transverse images when moving in a craniocaudal direction, where the ascending and descending portions of the thoracic aorta will not appear to be connected. The origin of the celiac artery can be used as the anatomical landmark between the descending thoracic aorta and abdominal aorta and the renal arteries serve as the anatomical landmark between the suprarenal and infrarenal segments of the abdominal aorta.
2. Arterial FDG uptake (as a measure of arterial inflammation) in the legs and neck is measured by placing a region of interest (ROI) around each artery of interest on slices of the coregistered transverse PET/CT images that pass through the artery. In the case of the aorta, beginning with the most superior aortic slice, carefully draw each ROI to include the entire area of FDG uptake on that slice while avoiding other surrounding tissues with increased radiotracer uptake (**Figure 1**). This image was taken from a patient in our aging and atherosclerosis study[20].
3. Next, using dedicated PET/CT image analysis software to calculate the SUV per slice [at our institution, we use Extended Brilliance Workstation, Philips Healthcare, Bothell, WA] the maximum and mean standardized uptake value (SUV) of each ROI is measured (**Figure 2**). This image was taken from a patient in our aging and atherosclerosis study[20].
4. Repeat this procedure for PET scan slices that pass through arteries of interest at regular intervals (e.g., every 5 - 20 mm). The total numbers of slices will differ from subject to subject depending on body habitus and anatomical variation.
5. Locate the inferior vena cava (IVC) in the abdomen where at least 6-8 contiguous slices can be visualized. Place an ROI around the IVC on each transverse slice to obtain at least 8 venous mean SUV measurements which will be used for tissue-to-background ratio (TBR) calculation as described later.

## 4. Imaging Outcome Calculations

1. Average arterial slice SUVs (using mean and maximum values) over all slices passing through an artery (e.g., carotid artery) or arterial segment of interest (e.g., ascending aorta, aortic arch, descending thoracic aorta, suprarenal abdominal aorta, infrarenal abdominal aorta) to generate mean SUV and maximum SUV measurements for each artery or arterial segment of interest. These parameters serve as one outcome measure of average burden of atherosclerosis within an artery or arterial segment of interest. Record the standard deviation of SUVs obtained from the slice measurements for statistical analyses.
2. Next, divide the arterial or arterial segment mean SUV by the venous mean SUV obtained in step 3.4 for normalization purposes. The result is an arterial or arterial segment TBR measure, which serves as another outcome for atherosclerotic plaque activity.
3. Finally, in an effort to understand the global burden of atherosclerotic disease within an artery or arterial segment of interest, multiply each arterial mean SUV obtained per slice ROI by the slice ROI volume (calculated by multiplying the area of the ROI by the slice thickness) and sum over all slices passing through an artery or arterial segment of interest. This yields arterial or arterial segment mean metabolic-volumetric product (MVP) as a third outcome for measurement of plaque activity and burden. Of note, regions in a vessel of interest that have no metabolic activity will contribute little to the MVP and therefore, this parameter is still valid as a measure of active plaque.
4. If one performs the summation of aortic mean MVPs listed in 4.3 over all slices passing through the aorta, the result will be the global inflammatory burden (GIB), which will serve as a fourth outcome for measurement of atherosclerotic plaque activity and atherosclerosis within the aorta.

An example of values for these four outcomes that have been derived from a single patient as part of an ongoing study[18] in psoriasis is shown in **Table 1**.

## 5. Representative Results

The table below shows various methods of determining outcomes for atherosclerotic plaque activity and vascular inflammation detected by FDG-PET/CT in a single patient with psoriasis.

| Arterial Segment (number of slices) | SUVmean (SD) | TBR (SD) | MVP (SD) | GIB(SD) |
|---|---|---|---|---|
| Ascending Aorta (n=8) | 1.43 (0.24) | 1.31 (0.18) | 5.68 (3.08) | 53.99 (19.50) |
| Aortic Arch (n=5) | 1.38 (0.25) | 1.30 (0.22) | 8.88 (4.94) | 59.85 (18.66) |

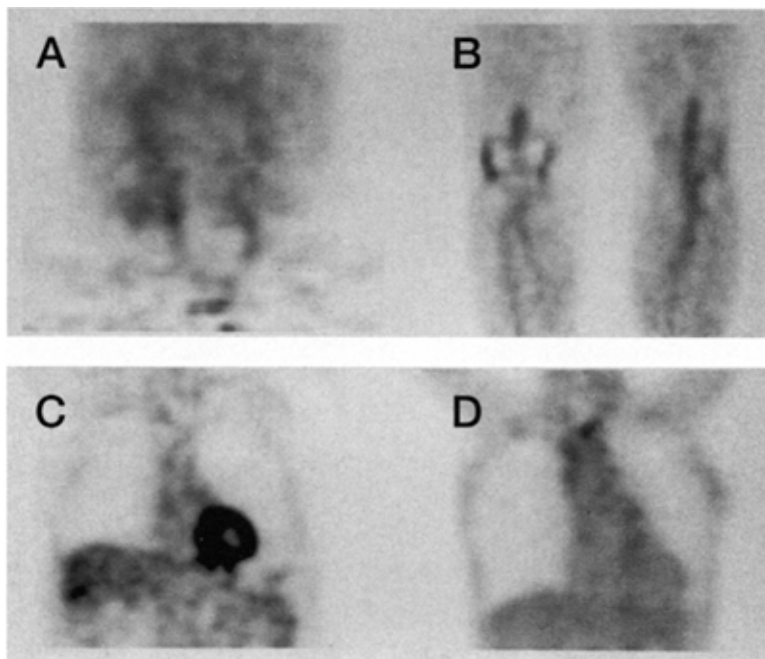| Descending Thoracic Aorta (n=20) | 1.42 (0.20) | 1.29 (0.19) | 3.11 (0.98) | 125.66 (53.11) |
|---|---|---|---|---|
| Suprarenal Abdominal Aorta (n=29) | 1.40 (0.19) | 1.26 (0.17) | 2.37 (0.66) | 50.75 (17.64) |
| Infrarenal Abdominal Aorta (n=26) | 1.38 (0.21) | 1.20 (0.16) | 1.72 (0.54) | 45.80 (10.86) |



**Figure 1.** PET images. A series of representative results of initial PET reconstruction images from a patient in our study of aging and atherosclerosis[20] which demonstrate FDG uptake in: A) the iliac and femoral arteries; B) popliteal arteries; C) abdominal aorta; D) aortic arch.



**Figure 2. Region of interest (ROI) placement.** A transverse fused FDG-PET/CT image is shown at the level of the proximal descending thoracic aorta from a patient in our study of aging and atherosclerosis[20]. The ROI is placed around the descending thoracic aorta, and the software will calculated mean SUV, maximum SUV, and area of ROI in mm[2]. This is for one slice of data through this arterial segment of interest, and the technique is then repeated for all slices passing through each segment of the aorta.

## Discussion

The methodology presented here is straightforward to perform, and can yield useful information regarding atherosclerotic plaque activity and vascular inflammation in clinically significant arterial beds. There are some important features of this analysis approach which warrant emphasis: 1) We use a high-quality PET/CT scanner which has 16 detector rows and with time of flight capability; 2) We utilize two experienced observers blinded to the clinical information to perform measurements to ensure consistency of the quantitative data; 3) We describe concurrently four outcomes of quantification which are each informative. We recommend measurement of at least arterial mean SUV and venous blood mean SUV so that TBR can be estimated. We believe that MVP, a novel quantitative parameter, will also be an important determinant of atherosclerotic plaque activity and vascular inflammation to obtain, as it provides global quantification of disease burden by incorporating structural and molecular measurements. SUV and TBR do not account for the structural changes observed in atherosclerotic vascular diseases, whereas MVP does. Furthermore, MVP allows for summation of multiple measurements obtained from a vessel of interest for purposes of global assessment.

PET/CT is ideally suited for assessment of the short and long term effects of therapeutic modulation of these outcomes given its high sensitivity, high contrast resolution, quantitative nature, and ability to provide combined metabolic and anatomical information. Future studies should examine the effects of standard and novel treatments beyond statin therapy upon vascular inflammation as measured by PET/CT, as well as upon other disease states associated with excess atherosclerosis such as metabolic syndrome, rheumatoid arthritis, and diabetes mellitus, so as to advance field of non-invasive detection, characterization, and treatment of the atherosclerosis plaque.

## Disclosures

No conflicts of interest declared.

## Acknowledgements

## References

1. Church, T.S., *et al.* Coronary artery calcium score, risk factors, and incident coronary heart disease events. *Atherosclerosis.* **190**, 224-231 (2007).
2. Kathiresan, S., *et al.* Assessment by cardiovascular magnetic resonance, electron beam computed tomography, and carotid ultrasonography of the distribution of subclinical atherosclerosis across Framingham risk strata. *Am. J. Cardiol.* **99**, 310-314, (2007).
3. Detrano, R., *et al.* Coronary calcium as a predictor of coronary events in four racial or ethnic groups. *N. Engl. J. Med.* **358**, 1336-1345 (2008).
4. Raggi, P., Cooil, B., Ratti, C., Callister, T.Q., & Budoff, M. Progression of Coronary Artery Calcium and Occurrence of Myocardial Infarction in Patients With and Without Diabetes Mellitus. *Hypertension.*, (2005).
5. Arad, Y., Goodman, K.J., Roth, M., Newstein, D., & Guerci, A.D. Coronary calcification, coronary disease risk factors, C-reactive protein, and atherosclerotic cardiovascular disease events: the St. Francis Heart Study. *J. Am. Coll. Cardiol.* **46**, 158-165 (2005).
6. Lorenz, M.W., Markus, H.S., Bots, M.L., Rosvall, M., & Sitzer, M. Prediction of clinical cardiovascular events with carotid intima-media thickness: a systematic review and meta-analysis. *Circulation.* **115**, 459-467 (2007).
7. Doherty, T.M., Detrano, R.C., Mautner, S.L., Mautner, G.C., & Shavelle, R.M. Coronary calcium: the good, the bad, and the uncertain. *Am. Heart. J.* **137**, 806-814 (1999).
8. Detrano, R. C., *et al.* Coronary calcium does not accurately predict near-term future coronary events in high-risk adults. *Circulation.* **99**, 2633-2638 (1999).
9. Chen, W., Bural, G.G., Torigian, D.A., Rader, D.J., & Alavi, A. Emerging role of FDG-PET/CT in assessing atherosclerosis in large arteries. *Eur. J. Nucl. Med. Mol. Imaging.* **36**, 144-151, doi:10.1007/s00259-008-0947-2 (2009).
10. Doherty, T.M., *et al.* Calcification in atherosclerosis: bone biology and chronic inflammation at the arterial crossroads. *Proc. Natl. Acad. Sci. U.S.A.* **100**, 11201-11206 (2003).
11. Fuster, V. & Lewis A. Conner Memorial Lecture. Mechanisms leading to myocardial infarction: insights from studies of vascular biology. *Circulation.* **90**, 2126-2146 (1994).
12. van der Wal, A.C., Becker, A.E., van der Loos, C.M., & Das, P.K. Site of intimal rupture or erosion of thrombosed coronary atherosclerotic plaques is characterized by an inflammatory process irrespective of the dominant plaque morphology. *Circulation.* **89**, 36-44 (1994).
13. van der Wal, A.C., Becker, A.E., van der Loos, C.M., Tigges, A.J., & Das, P.K. Fibrous and lipid-rich atherosclerotic plaques are part of interchangeable morphologies related to inflammation: a concept. *Coron. Artery Dis.* **5**, 463-469 (1994).
14. Alavi, A., *et al.* Positron emission tomography imaging of regional cerebral glucose metabolism. *Semin. Nucl. Med.* **16**, 2-34 (1986).
15. Hustinx, R., *et al.* Dual time point fluorine-18 fluorodeoxyglucose positron emission tomography: a potential method to differentiate malignancy from inflammation and normal tissue in the head and neck. *Eur. J. Nucl. Med.* **26**, 1345-1348 (1999).
16. Ogawa, M., *et al.* (18)F-FDG accumulation in atherosclerotic plaques: immunohistochemical and PET imaging study. *J. Nucl. Med.* **45**, 1245-1250 (2004).
17. Yun, M., *et al.* F-18 FDG uptake in the large arteries: a new observation. *Clin. Nucl. Med.* **26**, 314-319 (2001).
18. Mehta, N.N., *et al.* Systemic and Vascular Inflammation in Patients With Moderate to Severe Psoriasis as Measured by [18F]-Fluorodeoxyglucose Positron Emission Tomography-Computed Tomography (FDG-PET/CT): A Pilot Study. *Arch. Dermatol.* doi:10.1001/archdermatol.2011.119 (2011).
19. Davies, J.R., *et al.* FDG-PET can distinguish inflamed from non-inflamed plaque in an animal model of atherosclerosis. *Int. J. Cardiovasc. Imaging.* **26**, 41-48, doi:10.1007/s10554-009-9506-6 (2011).

20. Bural, G.G., *et al.* FDG-PET is an effective imaging modality to detect and quantify age-related atherosclerosis in large arteries. *Eur. J. Nucl. Med. Mol. Imaging.* **35**, 562-569, doi:10.1007/s00259-007-0528-9 (2008).

21. Arauz, A., Hoyos, L., Zenteno, M., Mendoza, R., & Alexanderson, E. Carotid plaque inflammation detected by 18F-fluorodeoxyglucose-positron emission tomography. Pilot study. *Clin. Neurol. Neurosurg.* **109**, 409-412 (2007).

22. Rominger, A., *et al.* 18F-FDG PET/CT identifies patients at risk for future vascular events in an otherwise asymptomatic cohort with neoplastic disease. *J. Nucl. Med.* **50**, 1611-1620 (2009).

23. Wasselius, J.A., Larsson, S.A., & Jacobsson, H. FDG-accumulating atherosclerotic plaques identified with 18F-FDG-PET/CT in 141 patients. *Mol. Imaging Biol.* **11**, 455-459, doi:10.1007/s11307-009-0223-2 (2009).

24. Tahara, N., *et al.* Simvastatin attenuates plaque inflammation: evaluation by fluorodeoxyglucose positron emission tomography. *J. Am. Coll. Cardiol.* **48**, 1825-1831 (2006).

25. Lee, S.J., *et al.* Reversal of vascular 18F-FDG uptake with plasma high-density lipoprotein elevation by atherogenic risk reduction. *J. Nucl. Med.* **49**, 1277-1282 (2008).

26. Rudd, J.H., *et al.* (18)Fluorodeoxyglucose positron emission tomography imaging of atherosclerotic plaque inflammation is highly reproducible: implications for atherosclerosis therapy trials. *J. Am. Coll. Cardiol.* **50**, 892-896 (2007).

27. Bural, G.G., *et al.* A pilot study of changes in (18)F-FDG uptake, calcification and global metabolic activity of the aorta with aging. *Hell. J. Nucl. Med.* **12**, 123-128 (2009).

28. Bural, G.G., *et al.* Quantitative assessment of the atherosclerotic burden of the aorta by combined FDG-PET and CT image analysis: a new concept. *Nucl. Med. Biol.* **33**, 1037-1043 (2006).